Available online at www.sciencedirect.com

ScienceDirect

Procedia Engineering 127 (2015) 1064 – 1070

Procedia Engineering

www.elsevier.com/locate/procedia

International Conference on Computational Heat and Mass Transfer-2015

# MHD Boundary Layer Flow of a Nanofluid Past a Wedge

D. Srinivasacharya[a,*], Upendar Mendu[b], K. Venumadhav[c]

[a]*Department of Mathematics, National Institute of Technology Warangal, Telangana - 506 004, India*
[b]*GITAM University, Hyderabad, Telangana - 502 329, India*
[c]*KITS Warangal, Telangana - 506 015, India*

**Abstract**

This paper analyzes the steady laminar magnetohydrodynamic (MHD) flow, heat and mass transfer characteristics in a nanofluid over a wedge in the presence of a variable magnetic field. The governing nonlinear partial differential equations are transformed into a system of ordinary differential equations using similarity variables and then solved numerically by using spectral quasi linearization method (SQLM). The present numerical results are validated by favourable comparisons with previously published ones as the special cases of the present investigations. The effects of magnetic parameter, Falkner-Skan power-law parameter and the volume fraction parameter on the non-dimensional heat and mass transfer rates are presented graphically.



Peer-review under responsibility of the organizing committee of ICCHMT – 2015

*Keywords:* Nanofluids; MHD; SQLM; Heat and Mass Transfer;

## 1. Introduction

The term ”nanofluid”, which is first pioneered by Chio et al. [1], to indicate engineered colloids, composed of nanoparticles dispersed in a base fluid for the enhancement of heat transfer rate. Chio noticed that the addition of one percent of nanoparticles by volume to the usual fluids increases the thermal conductivity of the fluid up to approximately twice. The state of art review of nanofluids is presented in the book by Das [2]. The flow, heat and mass transfer characteristics in nanofluids received the attraction of many researchers duo to its importance in industry and technology. Magnetic nanofluid is a magnetic colloidal suspension of carrier liquid and magnetic nanoparticles. The advantage of the magnetic nanofluid is that fluid flow and heat transfer can be controlled by an external source, which makes it applicable to various fields such as electronic packing, thermal engineering, and aerospace. On the other hand, the study of magneto-hydrodynamic flow for an electrically conducting fluid past a heated wedge has important applications in many engineering problems such as plasma studies, petroleum industries, MHD power generators, cooling of nuclear reactors, the boundary layer control in aerodynamics, and crystal growth. Further, MHD is significant in the control of boundary layer flow and metallurgical processes. Several authors ([3–9]) studied the effects of MHD on laminar boundary layer flow, heat and mass transfer over a wedge in different situations for

* D. Srinivasacharya. Tel.: +91-2462821 ; fax: +91-870-2459547.
*E-mail address:* dsc@nitw.ac.in, dsrinivasacharya@gmail.com



Peer-review under responsibility of the organizing committee of ICCHMT – 2015
doi:10.1016/j.proeng.2015.11.463

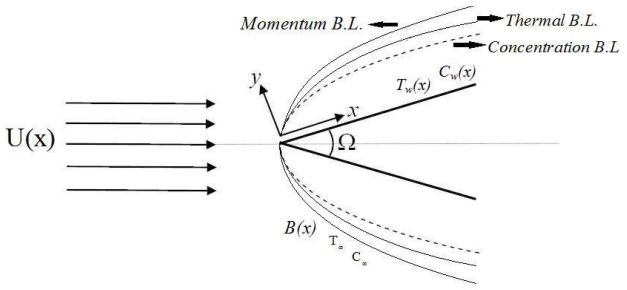


Fig. 1. Physical model and coordinate system.

different types of fluids. Makanda [10] studied that the natural convection of viscoelastic fluid from a cone embedded in a porous medium with viscous dissipation.

Papailiou and Lykoudis [11], established experimentally the existence of the similarity solutions for the case of variable magnetic field. They found that similarity solutions exist when the intensity of the magnetic field changes with, where is the coordinate measured in the direction of the flow. The objective of this paper is to consider the effect of variable magnetic field on the fluid flow and heat transfer characteristics for a fixed wedge with variable wall temperature and concentration.

## 2. Mathematical Formulation

Consider a steady laminar boundary layer flow past a wedge embedded in a free stream of electrically conducting nanofluid with velocity U(x). Choose the co-ordinate system such that x-axis is along the surface of the wedge andy-axis normal to the surface of the wedge, as shown in the Fig. 1. The surface of the wedge is maintained with variable temperature Tw(x) and variable concentrationCw(x). T and C are ambient temperature and concentration at any arbitrary reference point in the medium, respectively. A variable magnetic field B(x) is applied normal to the walls of the wedge. The magnetic Reynolds number is assumed to be small so that the induced magnetic field can be neglected in comparison with the applied magnetic field. With the above assumptions, using Boussinesq and boundary layer approximations, the governing equations for the nanofluid flow are given by

$$\frac{\partial u}{\partial x} + \frac{\partial u}{\partial y} = 0 \tag{1}$$

$$u\frac{\partial u}{\partial x} + v\frac{\partial u}{\partial y} = U(x)\frac{dU(x)}{dx} + \frac{\mu_{nf}}{\rho_{nf}}\frac{\partial^2 u}{\partial y^2} + \frac{\sigma B(x)^2}{\rho_{nf}}(U(x) - u), \tag{2}$$

$$u\frac{\partial T}{\partial x} + v\frac{\partial T}{\partial y} = \alpha_{nf}\frac{\partial^2 T}{\partial y^2}, \tag{3}$$

$$u\frac{\partial C}{\partial x} + v\frac{\partial C}{\partial y} = D_1\frac{\partial^2 C}{\partial y^2}. \tag{4}$$

where $u$ and $v$ are the components of velocity along $x$ and $y$ directions respectively, $T$ is the dimensional temperature of the fluid near the plate, $C$ is the dimensional concentration, $D_1$ is the molecular diffusivity of nanofluid.

The effective dynamic viscosity($\mu_{nf}$), the effective density($\rho_{nf}$), the thermal diffusivity ($\alpha_{nf}$) and heat capacitance ($(\rho C_p)_{nf}$) of the nanofluid are given by

$$\mu_{nf} = \frac{\mu_f}{(1-\phi)^{2.5}}, \quad \rho_{nf} = (1-\phi)\rho_f + \phi\rho_s, \quad \alpha_{nf} = \frac{k_{nf}}{(\rho C_p)_{nf}}, \quad (\rho C_p)_{nf} = (1-\phi)(\rho C_p)_f + \phi(\rho C_p)_s. \tag{5}$$

where $\phi$ is the solid volume fraction of nanoparticles. The thermal conductivity of nanofluids restricted to spherical nanoparticles is approximated by the Maxwell-Garnetss (MG) model (see [12] and [13]),

$$k_{nf} = k_f \, \frac{k_s + 2k_f - 2\phi(k_s + k_f)}{k_s + 2k_f + \phi(k_s + k_f)} \tag{6}$$

Here, the subscript $nf$, $f$ and $s$ represent the thermophysical properties of the nanofluid, base fluid and nano solid particles, respectively.

The boundary conditions are:

$$\begin{array}{l} u = 0, \quad v = 0, \quad T = T_w(x), \quad C = C_w(x) \quad \text{at} \quad y = 0, \\ u \to U(x) = u_0 \, x^m, \quad T \to T_\infty, \quad C \to C_\infty \quad \text{as} \quad y \to \infty, \end{array} \tag{7}$$

The aim of this study is to estimate the skin friction coefficient $C_f$ , local heat transfer coefficient, Nusselt number $Nu_x$ and local mass transfer coefficient, Sherwood number$Sh_x$. These are defined as

$$C_f = \frac{\mu_{nf}}{\rho(U(x))^2} \left(\frac{\partial u}{\partial y}\right)_{y=0}, \; Nu_x = \left(\frac{k\,x}{k_f\,(T_w(x) \, - \, T_\infty)}\right)\left(\frac{\partial T}{\partial y}\right)_{y=0}, \; Sh_x = \frac{x}{(C_w(x) - C_\infty)} \left(\frac{\partial C}{\partial y}\right)_{y=0} \tag{8}$$

Hence, the non dimensional skin friction coefficient, local heat-transfer coefficient and mass transfer coefficient are given by

$$(1-\phi)^{2.5} \, \sqrt{Re_x} C_f = 2 \; F''(0), \; \frac{Nu_x}{\sqrt{Re_x}} \frac{k_f}{k_{nf}} = -\theta'(0), \; \frac{Sh_x}{\sqrt{Re_x}} = -\phi'(0) \tag{9}$$

where the local Reynolds number $Re_x = \dfrac{x\,U(x)}{\nu_f}$.

## 3. Method of solution

In order to obtain similarity solutions of the problem, we assume that the variable magnetic field $B(x)$ is of the form $B(x) = B_0 x^{(m-1)/2}$, where $B_0$ is the uniform magnetic field (see [14],[15]). Further, we assume that the free stream velocity $U(x)$ is of the form $U(x) = U_0 x^m$, where $u_0$ is constant and $m$ is the Falkner-Skan power-law parameter with $0 \leqslant m \leqslant 1$. Here $m = \beta/(2-\beta)$ where $\beta$ is the Hartree pressure gradient parameter that corresponds to $\beta = \Omega/\Pi$ for the total wedge angle $\Omega$. We note that $\beta = 0$ and $\beta = 1$ correspond to the horizontal and vertical wall cases, respectively.

Introducing the stream function $\psi(x, y)$ through $u = \dfrac{\partial \psi}{\partial y}$, $v = -\dfrac{\partial \psi}{\partial x}$ and the following similarity variables

$$\left.\begin{array}{l} \psi = (\nu_f \, u_0 \, x^{m+1})^{1/2} F(\eta), \quad \eta = \left(\dfrac{u_0 \, x^{m+1}}{\nu_f}\right)^{1/2} \dfrac{y}{x}, \; \dfrac{T - T_\infty}{T_w(x) - T_\infty} = \theta(\eta), \; T_w(x) - T_\infty = x\,\Delta T \\ \dfrac{C - C_\infty}{C_w(x) - C_\infty} = \phi(\eta), \quad C_w(x) - C_\infty = x\,\Delta C \end{array}\right\}. \tag{10}$$

in Eqs. (2), (3) and (4), we obtain

$$F''' - \phi_1 \left[ m\,F'^2 - \left(\frac{m+1}{2}\right) F\,F'' - m \right] + (1-\phi)^{2.5} \, M \, (1 - F') = 0, \tag{11}$$

$$\theta'' + Pr \, \frac{k_f}{k_{nf}} \, \phi_2 \left( \frac{m+1}{2} \, F\,\theta' - F'\,\theta \right) = 0, \tag{12}$$

$$\varphi'' + Sc \left( \frac{m+1}{2} \, F\,\varphi' - F'\,\varphi \right) = 0, \tag{13}$$

where a prime denotes differentiation with respect to $\eta$, $Pr = \dfrac{\nu_f(\rho C_p)_f}{k_f}$ is the Prandtl number, $Sc = \dfrac{\nu_f}{D}$ is the Schmidt number and $M = \dfrac{\sigma {B_0}^2}{\rho_{nf} u_0}$ is the magnetic parameter, $\phi_1 = (1-\phi)^{2.5}\left[1-\phi+\phi\dfrac{\rho_s}{\rho_f}\right]$, $\phi_2 = \left[1-\phi+\phi\dfrac{(\rho C_p)_s}{(\rho C_p)_f}\right]$.

The boundary conditions (7) in terms of $F$, $\theta$ and $\varphi$ becomes

$$\left.\begin{array}{ll} \eta = 0: & F(0)=0, F'(0)=0, \theta(0)=1, \varphi(0)=1, \\ as \quad \eta\to\infty: & F'\to 1, \quad \theta\to 0, \quad \varphi\to 0, \end{array}\right\}. \tag{14}$$

## 4. The Spectral QLM Solution of the Problem

The non-linear nonhomogeneous differential equations (11) - (13) are solved subject to the boundary conditions (14) numerically using the spectral quasi- linearization method [16]. Applying the Quasi Linearization Method (QLM) on Eqs. (11) - (13) gives the following iterative sequence of linear differential equations,

$$F'''_{r+1} + a_{1,r}F''_{r+1} + a_{2,r}F'_{r+1} + a_{3,r}F_{r+1} = a_{4,r}, \tag{15}$$

$$b_{1,r}F'_{r+1} + b_{2,r}F_{r+1} + \theta''_{r+1} + b_{3,r}\theta'_{r+1} + b_{4,r}\theta_{r+1} = b_{5,r}, \tag{16}$$

$$c_{1,r}F'_{r+1} + c_{2,r}F_{r+1} + \varphi''_{r+1} + c_{3,r}\varphi'_{r+1} + c_{4,r}\varphi_{r+1} = c_{5,r}, \tag{17}$$

where the coefficients $a_{is,r}, (s = 1,2,3,4)$, $b_{i,r}$ and $c_{i,r}$, $(i = 1,2,3,4,5)$ are known functions (from previous calculations) and are defined as

$$a_{1,r} = \phi_1\frac{m+1}{2}F_r, \quad a_{2,r} = -2m\phi_1 F'_r, \quad a_{3,r} = \phi_1\frac{m+1}{2}F''_r,$$

$$a_{4,r} = -\phi_1 m - \frac{M}{\phi_3}(1-\phi)^{2.5} - \phi_1 m(f'_r)^2 - \phi_1\frac{m+1}{2}F_r F''_r, \quad b_{1,r} = -Pr\,\phi_2\frac{k_f}{k_{nf}}\theta_r, \quad b_{2,r} = Pr\,\phi_2\frac{k_f}{k_{nf}}\frac{m+1}{2}\theta'_r,$$

$$b_{3,r} = Pr\,\phi_2\frac{k_f}{k_{nf}}\frac{m+1}{2}F_r, \quad b_{4,r} = -Pr\,\phi_2\frac{k_f}{k_{nf}}F'_r, \quad b_{5,r} = -Pr\,\phi_2\frac{k_f}{k_{nf}}(\theta_r F'_r - \frac{m+1}{2}F_r\theta'_r),$$

$$c_{1,r} = -Sc\,\varphi_r, \quad c_{2,r} = Sc\,\frac{m+1}{2}\varphi'_r, \quad c_{3,r} = Sc\,\frac{m+1}{2}F_r, \quad c_{4,r} = -Sc\,F'_r, \quad c_{5,r} = -Sc\,(\varphi_r F'_r - \frac{m+1}{2}F_r\varphi'_r).$$

The above QLM sceme (15) to (17) is a coupled linear system of differential equations with variable coefficients, and is ready to solve iteretively using any numerical method such as finite differences, finite elements, Runge-Kutta based shooting methods or collocation methods for r = 1, 2, 3.... In this work, as will be discussed below, the Chebyshev spectral collocation method was used to solve the QLM scheme (15) to (17). This method is based on approximating the unknown functions by the Chebyshev interpolating polynomials in such a way that they are collocated at the Gauss-Lobatto points defined as

$$\eta_j = cos(\frac{j\pi}{N}), j = 0,1,2...,N, \tag{18}$$

where $N$ is the number of collocation points used. The derivative of $F_{r+1}$ at the collocation points are represented as

$$\frac{d^s F_{r+1}}{d\eta^s} = \sum_{k=0}^{N} D^s_{kj}F_{r+1}(\eta_k) = \mathbf{D}^s\,\mathfrak{F} \quad j = 0,1,2,...,N, \tag{19}$$

where $D^s = ((2/L)\mathfrak{D})^s$ and $\mathfrak{D}$ is the Chebyshev spectral differentiation matrix (see, e.g., [20, 21]), and $\mathfrak{F}$ is the vector function is given by $\mathfrak{F} = [F(\eta_0), F(\eta_1), ..., F(\eta_N)]^T$. Similarly the derivatives of $\theta$ and $\varphi$ are given by $\theta^{(s)} = \mathbf{D}^s\,\Theta$ and $\varphi^{(s)} = \mathbf{D}^s\,\Phi$, where $s$ is the order of derivative, and $\mathbf{D}$ is the matrix of order $(N+1)\times(N+1)$. Substituting (18) and (19) in SQLM scheme (15) - (17) results in the following matrix equation

$$\begin{bmatrix} A_{11} & A_{12} & A_{13} \\ A_{21} & A_{22} & A_{23} \\ A_{31} & A_{32} & A_{33} \end{bmatrix}\begin{bmatrix} \mathfrak{F}_{r+1} \\ \Theta_{r+1} \\ \Phi_{r+1} \end{bmatrix} = \begin{bmatrix} K_1 \\ K_2 \\ K_3 \end{bmatrix}, \tag{20}$$

where

$$A_{11} = \mathbf{D}^3 + a_{1,r}\mathbf{D}^2 + a_{2,r}\mathbf{D} + a_{3,r}\mathbf{I}, \qquad A_{12} = \mathbf{O}, \qquad A_{13} = \mathbf{O},$$
$$A_{21} = b_{1,r}\mathbf{D} + b_{2,r}\mathbf{I}, \qquad A_{22} = \mathbf{D}^2 + b_{3,r}\mathbf{D} + b_{4,r}\mathbf{I}, \qquad A_{23} = \mathbf{O}, \tag{21}$$
$$A_{31} = c_{1,r}\mathbf{D} + c_{2,r}\mathbf{I}, \qquad A_{23} = \mathbf{O}, \qquad A_{33} = \mathbf{D}^2 + c_{3,r}\mathbf{D} + c_{4,r}\mathbf{I},$$
$$\mathbf{K_1} = a_{4,r}, \qquad \mathbf{K_2} = b_{5,r}, \qquad \mathbf{K_3} = c_{5,r}.$$

In the above definitions, $a_{s,r}(s = 1, 2, 3)$, $b_{i,r}$ and $c_{i,r}$, $(i = 1, 2, 3, 4, 5)$ are diagonal matrices of size $(N + 1) \times (N + 1)$, $\mathbf{I}$ is a $(N + 1) \times (N + 1)$ identity matric and $\mathbf{O}$ is a matrix of zeroes of order $(N + 1) \times (N + 1)$. The approximate solutions for $\mathfrak{F}, \Theta$ and $\Phi$ are obtained by solving the matrix system (20).

## 5. Results and Discussion

The nonlinear differential equations (11) - (13) with boundary conditions (14) do not have a closed form solution. These equations were solved numerically using the SQLM. To check the accuracy of the solutions, the non-dimensional skin friction for pure water (nanoparticle volume fraction ) is compared with results reported by Ariel (1994) for the case of vertical plate , and it was found that they are in good agreement.

Table 1. Comparison of skin friction $F''(0)$ values calculated by the present method and that of [17], for pure water $\phi = 0$, $m = 1$, with $Pr = 1$ and $Sc = 0.24$.

| M | [17] | Present |
|---|---|---|
| 0 | 1.232588 | 1.2325965196 |
| 1 | 1.585331 | 1.5852800424 |
| 4 | 2.346663 | 2.3468696599 |
| 25 | 5.147965 | 5.1479646032 |
| 100 | 10.074741 | 10.0747411168 |

In the present work, MHD mixed convection heat and mass transfer past a wedge immersed in water based nanofluid with variable wall temperature and concentration is conducted. In this study, two different nanoparticles, namely, silver ($Ag$) and gold ($Au$), with water as the base fluid considered. The Prandtl number of the base fluid was kept at constant as $Pr = 6.7850$. The thermophysical properties of the nanofluid are given in table 2 (see Oztop and Abu-Nada [18]).

Table 2. Thermo-physical properties of water and nanoparticles.

| *Properties* | $\rho(kg/m^3)$ | $C_p(J/kg\,K)$ | $k(W/mK)$ |
|---|---|---|---|
| Pure water | 997.1 | 4179 | 0.613 |
| Ag | 10500 | 235 | 429 |
| Au | 19282 | 129 | 310 |

Volume fraction of nanoparticles is a key parameter for studying the effect of nanoparticles on flow fields, temperature and concentration distributions of nanofluids, the resulting influence of $\phi$ on the non-dimensional profiles is presented in the Figs. 2, for both $Ag - water$ and $Au - water$ nanofluids. In the limiting case $\phi \to 0$ corresponds to the base fluid (water). In Fig. 2 the velocity across the boundary layer is shown for different values of the nanoparticle volume fraction. From Fig. 2(a) velocity of both types of nanofluids increase for the increasing values of $\phi$. As the nanoparticle volume fraction $\phi$ increases, in the dynamic boundary layer the width of the velocity profiles decreases, because of the gradient of the velocity from wall to free stream is more rapid when $\phi$ increases. The same trend is observed in the case of a $Au - water$ nanofluid. Figs. 2(b) and 2(c) illustrate the effect of the nanoparticle volume fraction on the temperature and concentration profiles, respectively, in the case of a $Ag - water$ nanofluid. It is clear

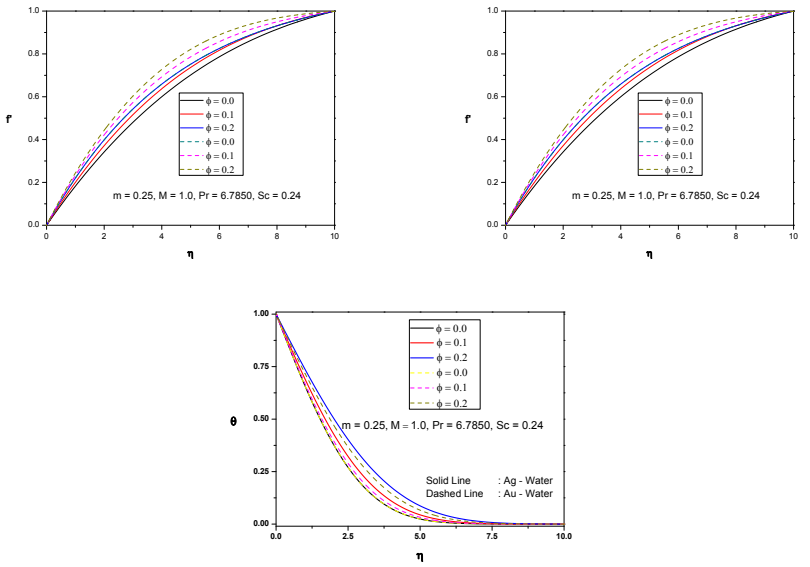


Fig. 2. (a) Velocity ; (b) Temperature and (c) Concentration profiles for different values of $\phi$

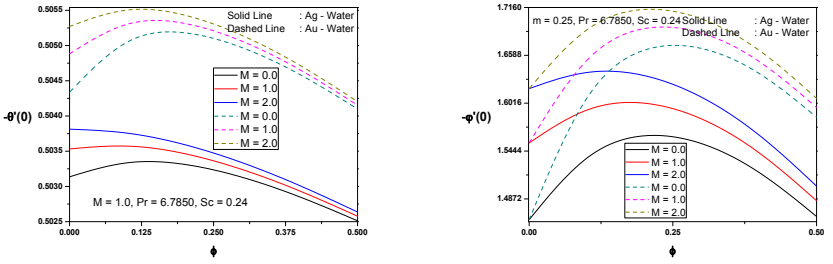


Fig. 3. Effect of $M$ on (a) Heat transfer rate; (b) Mass transfer rate

that as the nanoparticle volume fraction increases the nanofluid temperature and the concentration increase. This can be explained as the thermal conductivity of the nanofluid increases as the solid nano particles increase which are having the high thermal conductivity than the base fluid. Hence, the heat transfer from base fluid to solid nano particles is more and increases the temperature of the nanofluid. Since the thermal conductivity of $Ag$ is more than that of $Au$, hence, for the increasing solid nano particles of $Ag$ and $Au$ in the base fluid, we observe that the temperature distribution of $Ag - water$ nanofluid is correspondingly higher than that of a $Au - water$ nanofluid. As a result, the temperature of the nanofluid increases in mixed convection, with increasing nanoparticle volume fraction. Same trend can be seen in the case of $Au - water$ nanofluid. The concentration boundary layer thickness increases for both types of nanofluids. And further we can conclude that the velocity, temperature and concentration profiles of nanofluids are higher than that of the water ($\phi = 0$ corresponds to the base fluid (water)).

Figure (3) depict the variation of heat transfer rate (local Nusselt number ($Nu_x$)), mass transfer rate (local Sherwood number ($Sh_x$)) with volume fraction of nanoparticles ($\phi$) for different values of magnetic parameter ($M$) of both water based nanofluids. It is seen that both the local Nusselt number and local Sherwood number increase as the magnetic parameter increases. This is due to the motive force created by traverse magnetic field which tends to accelerate the flow. As explained above, the nanofluid velocity increases as the magnetic parameter ($M$) increases in the mixed convection, as a result of the hot nanofluid replaced by the cooled nanofluid chunks, hence the higher heat transfer rates can be seen. A similar analogy con be seen in mass transfer rate.

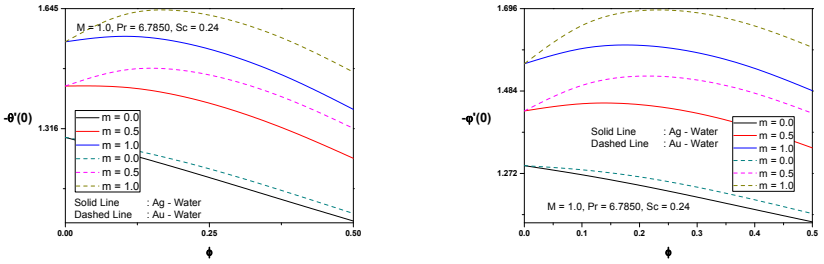


Fig. 4. Effect of $m$ on (a) Heat transfer rate; (b) Mass transfer rate

Figs. 4 (a) and (b) show the heat transfer and mass transfer coefficients as a function of nanoparticle volume fraction $\phi$ for $m = 0$ (horizontal plate), $m = 0.5$ (wedge surface) and $m = 1$ (stagnation point flow). As the wedge angle parameter is increased, the local Nusselt number and the local Sherwood number increase for forced convection. This may be explained by the fact that as the wedge angle increases, the wedge becomes flatter and less of an obstruction. It is worth noting that the present study reduces to that of a regular viscous fluid when $\phi = 0$.

The variation of the wall heat and mass transfer rates are shown for different values of nanoparticle volume fraction and for different configurations of the wedge surface in Figs. 3 - 4. The heat and mass transfer rates more for the increasing values of $\phi$. The heat and mass transfer rates increase from pure base fluid ($\phi \to 0$) to that of nanofluid. Same trends can be seen in both the water based nanofluids.

## References

[1] Stephen U. S. Choi, J. A. Eastman, Enhancing thermal conductivity of fluids with nanoparticles, ASME International Mechanical Engineering Congress & Exposition, San Francisco, CA, November, (1995) 12–17.
[2] S. K. Das, S. U. S. Choi, W. Yu, T. Pradeep, Nanofluids: Science and Technology, John Wiley & Sons, New York, 2008.
[3] AnuarIshak, RoslindaNazar, Ioan Pop, MHD boundary - layer flow of a micropolar fluid past a wedge with constant wall heat flux, Commun. Nonlinear Sci. Numer. Simul. 14 (2009) 1091–18.
[4] T. Hayat, Majid Hussain, Nadeem, S. Meslou, Falkner-Skan wedge flow of a power-law fluid with mixed convection and porous medium, Computers & Fluids, 49, (2011). 22–28.
[5] Kai-Long Hsiao, MHD mixed convection for viscoelastic fluid past a porous wedge, Int. J. Non Linear Mech. 46, (2011) 1-8.
[6] R. Kandasamy, I. Hashim, Muhaimin, Seripah, Nonlinear MHD mixed convection flow and heat and mass transfer of first order chemical reaction over a wedge with variable viscosity in the presence of suction or injection. Theoret. Appl. Mech.34(2), (2007) 111–134.
[7] Md Shakhaoath Khan, Ifsana Karim, MdSirajul Islam, Mohammad Wahiduzzaman, MHD boundary layer radiative, heat generating and chemical reacting flow past a wedge moving in a nanofluid, Nano Convergence, 1:20 (2014).
[8] W. N. Mutuku-Njane, O. D. Makinde, MHD nanofluid flow over a permeable vertical plate with convective heating, Journal of Computational and Theoretical Nanoscience, 11(3), (2014)667–675.
[9] K. V. Prasad, P. S. Datti, K. Vajravelu, MHD mixed convection flow over a permeable non-isothermal wedge, Journal of King Saud University Science, 25, (2013) 313–324.
[10] G. Makanda, O. D. Makinde, P. Sibanda, Natural convection of viscoelastic fluid from a cone embedded in a porous medium with viscous dissipation, Mathematical Problems in Engineering, 2013, 934712.
[11] D. D. Papailiou, P. S. Lykoudis, Magneto-fluid-mechanic laminar natural convection an experiment. Int J Heat Mass Transfer, 11, (1968) 138–591.
[12] J. C. Maxwell Garnett, Philos. Trans. R. Soc. London A 203, (1904) 385.
[13] C. A. Guerin, P. Mallet, A. Sentenac, Effective medium theory for finite size aggregates, J. Opt. Soc. Am. A 23, (2006) 349–35841.
[14] M. H. Cobble, Magneto fluid dynamic flow with a pressure gradient and fluid injection, J. Engng. Math. 11(2), (1977) 49–56.
[15] Z. Zhang,J. Wang, Exact self-similar solutions of the magnetohydrodynamic boundary layer system for power-law fluids. Z Angew Math Phys.58, (2007) 805–817.
[16] S.S. Motsa, P. Sibanda, Some modifications of the quasilinearization method with higher-order convergence for solving nonlinear BVP's, Numer. Algor. 63, (2013) 399–417.
[17] P. D. Ariel, Hiemnz flow in hydromagnetics, Acta Mech., 103, (1994) 31–43.
[18] H. F. Oztop, E. Abu-Nada, Numerical study of natural convection in partially heated rectangularenclosures filled with nanofluids. Int. J. Heat Fluid Flow, 29, (2008) 13-26.